Journal of Arid Environments 236 (2026) 105651

Contents lists available at ScienceDirect

Journal of Arid Environments

journal homepage: www.elsevier.com/locate/jaridenv

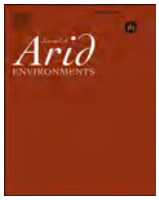

Topography-mediated aboveground biomass (AGB) carbon storage in semiarid Patagonia: native forests and pine plantations at the landscape scale

Tatiana Alejandra Valfré-Giorello [a,b,c,*], Lisandro Agost [d], Georgina Conti [e], Carla Montero [c], Maria Elena Oneto [c], Daniel Roberto Pérez [a]

[a] Universidad Nacional del Comahue. Facultad de Ciencias del Ambiente y la Salud. Laboratorio de Rehabilitación y Restauración de Ecosistemas Áridos y Semiáridos (LARREA), Buenos Aires 1400. CP, Neuquén, 8300, Argentina
[b] Consejo Nacional de Investigaciones Científicas y Técnicas (CONICET), Argentina
[c] Y-TEC, . Av. del Petróleo Argentino 900-1198, Berisso, Buenos Aires, B1923, Argentina
[d] Universidad Nacional de Córdoba. Centro de Ecología y Recursos Naturales Renovables "Dr. Ricardo Luti" (CERNAR), Av. Vélez Sarsfield 1611, Córdoba, X5016GCA, Argentina
[e] Universidad Nacional de Córdoba. Instituto Multidisciplinario de Biología Vegetal (IMBIV-CONICET), Av. Vélez Sarsfield 1611, Córdoba, X5016GCA, Argentina

ARTICLE INFO

Keywords:
Climate change
GEDI
Random forest regression
SAR
Species richness

ABSTRACT

Accurate mapping of forest carbon stocks and biodiversity is critical for guiding conservation and climate mitigation strategies, particularly in topographically complex mountain regions. We integrated remote sensing data (optical, SAR, LiDAR), topographic variables, and field inventories into a Random Forest Regression using a Nested cross-validation framework to model AGB carbon stock across native forests and pine plantations in the semiarid Andean Patagonia. Specifically, we aimed to: (i) classify vegetation types; (ii) estimate AGB carbon stock and uncertainty; (iii) map the effects of vegetation and topography on AGB carbon stock; and (iv) compare understory biodiversity among vegetation. The model achieved moderate to high performance ($R^2 = 0.78$, *RMSE* % = 33.86%). Pine plantations and native forest had significant differences in AGB carbon, but at mid elevations (1400–1500 m a.s.l.) and gentle slopes (0–10°)-, both stored comparable values (100 Mg C ha^{-1}). Native forests supported higher biodiversity than pine plantations (species richness: 4.60 ± 0.34 vs.0.10 ± 0.07, respectively), and occupied a broader topographic range. Elevation and slope emerged as key drivers shaping the spatial distribution of AGB carbon storage for both vegetation. Management strategies should prioritize the conservation and restoration of native forests in topographic settings where they achieve high AGB carbon stocks while sustaining endemic biodiversity.

1. Introduction

Global climate change represents one of the most pressing challenges of our time, with current and projected impacts on natural systems and human societies requiring effective mitigation strategies (IPCC, 2014). Among the proposed actions, "natural climate solutions" include the conservation of native ecosystems as well as restoration practices aimed at enhancing ecosystem productivity (Griscom et al., 2017; Ameray et al., 2021; Pan et al., 2024). Forests are central to these strategies due to their capacity to sequester and store carbon over the long term, their role as major reservoirs of biodiversity, and their vulnerability to disturbances that can release substantial amounts of carbon back to the atmosphere (Hua et al., 2022; Pan et al., 2024).

Afforestation practices involving species outside their natural range are expanding globally, driven by climate policy and carbon credit markets (Tudor et al., 2025). Exotic conifers, particularly *Pinus* species, have been widely promoted for their rapid growth (Richardson and Rejmánek, 2004). However, in the drylands of Argentine Patagonia, non-native *Pinus* plantations achieve productivity levels comparable to native forest species, and their growth may respond more negatively to climate warming (Reiter et al., 2025). In addition, these plantations generate multiple socio-ecological costs, including invasive spread,

* Corresponding author. Universidad Nacional del Comahue. Facultad de Ciencias del Ambiente y la Salud. Laboratorio de Rehabilitación y Restauración de Ecosistemas Áridos y Semiáridos (LARREA), Buenos Aires 1400. CP, Neuquén, 8300, Argentina.
E-mail address: tvalfregiorello@gmail.com (T.A. Valfré-Giorello).

https://doi.org/10.1016/j.jaridenv.2026.105651
Received 11 September 2025; Received in revised form 22 April 2026; Accepted 12 May 2026
Available online 19 May 2026

increased fire risk, high water use, and biodiversity loss (Brockerhoff et al., 2008; Simberloff et al., 2010), although they may provide short-term carbon gains due to harvest cycles (Ameray et al., 2021) and rapid carbon turnover (Araujo and Austin, 2020). By contrast, native forests can sustain long-term carbon storage through continuous biomass accumulation across life stages, including in old-growth trees (Körner, 2017), while simultaneously supporting biodiversity conservation, water regulation, and cultural values (Díaz et al., 2018). These contrasts highlight the need to critically evaluate the potential and limitations of plantation-based approaches relative to native forest conservation.

At the landscape scale, topography influences the spatial distribution of forest carbon stocks (Wang et al., 2019; Zhao et al., 2023). Elevation, slope, and aspect influence local environmental conditions such as temperature, rainfall, solar radiation, water availability, and multiple soil properties (Körner, 1999). These variables, in turn, affect forest structure and productivity, thereby regulating carbon accumulation across the landscape (Zhao et al., 2023; Xu et al., 2023). The magnitude and direction of topographic effects on carbon storage vary with regional climate and soil characteristics, making their explicit consideration essential for site-level planning and forest management (Zhengchao et al., 2016). Despite their importance, large-scale carbon accounting models often overlook or inadequately represent the combined effects of topographic variables.

Remote sensing technologies can overcome traditional limitations of forest inventories by enabling large-area assessments; however, their accuracy depends on robust correlations between sensor responses and target variables, which may vary across forest types and topographic gradients. Optical sensors quantify biophysical parameters but are subject to spectral saturation in dense canopies (Mutanga et al., 2023). In contrast, synthetic aperture radar (SAR) data can capture vertical structure through backscatter (e.g., canopy height, leaf area index) but are limited by signal saturation at C-band in dense vegetation (Moreira et al., 2013). Spaceborne LiDAR provides detailed vertical profiles but has sparse spatial coverage (Dubayah et al., 2020). Integrated approaches combining optical, SAR, and LiDAR data have the potential to improve predictions of carbon stocks and forest structure but they must address challenges such as resolution mismatches and terrain-induced errors (Dong et al., 2024).

Within this context, machine learning algorithms, such as Random Forest, provide a flexible framework for integrating field measurements with multi-sensor remote sensing data, accommodating non-linear relationships, identifying key predictors, and handling noise (Breiman, 2001). These approaches may be particularly relevant in complex terrains, where topography affects both ecological processes and the quality of remotely sensed signals through distortion and shadowing effects in SAR and LiDAR data (Luo et al., 2025). As a result, modelling frameworks that incorporate topographic variability are likely to improve the spatial characterization of carbon stocks. Despite these advances, challenges persist in establishing long-term baselines across regions, particularly in heterogeneous landscapes.

Understanding the quantity and spatial distribution of aboveground biomass carbon stocks (hereafter, AGB carbon), as well as the topographic variables that regulate them, is crucial for evaluating the effectiveness of afforestation projects and developing effective forest management strategies. In this study, we integrated a Random Forest regression model with field measurements and multi-source remote-sensing data to estimate AGB carbon stocks in native forests and pine plantations in the mountains of northwestern Patagonia. Specifically, we aimed to: (i) perform a land cover classification of forest types; (ii) assess the performance of multisensor predictors in estimating AGB carbon stocks, including associated uncertainty; (iii) quantify and map the effects of vegetation and topography on AGB carbon stocks. We included an additional objective to evaluate one of the main consequences identified for Pinus plantations: biodiversity loss. To achieve this, (iv) we compared understory plant diversity in forest plantations and in adjacent native forests, and explored the potential ecological implications of these differences.

2. Methods

2.1. Study area

This study focuses on an area in the Cordillera Norte (Bran et al., 2002), an Andean region of northwestern Patagonia, Argentina (36°50′ S, 70°50” W, Minas department, Neuquén province; Fig. 1A), with an elevation ranging from 1200 to 3000 m a.s.l. The climate is Mediterranean, characterized by cold, humid winters and warm, dry summers (Paruelo et al., 1998). The average annual temperature is 10 °C. Precipitation ranges from 600 to 1000 mm yr^{-1}, with a west-to-east gradient, occurring as rain and snow (Movia et al., 1982; Paruelo et al., 1998). The predominant soil type is Andisol, an acidic soil derived from volcanic ash. These soils are predominantly sandy-loam textured and exhibit seasonal summer water deficits. In low-lying areas adjacent to rivers, streams, and drainage channels (wetlands), deep, moist soils prevail, with finer textures, high organic matter content, and a shallow water table (Bran et al., 2002), reflecting a marked topographic complexity that characterizes these forested landscapes.

The vegetation corresponds to a mosaic of Patagonian, High Andean, and Subantarctic phytogeographic provinces (Movia et al., 1982), and is dominated by grass steppes and shrublands with fragmented remnant native forests of *Nothofagus antarctica* embedded within more protected environments (Fig. 1B). The region's primary economic activities include extensive sheep and goat grazing and, more recently, pine plantations, both of which have contributed to desertification and altered carbon stocks (Laclau, 2003; Mendez-Casariego et al., 2005). Plantations consist of *Pinus ponderosa* and *P. contorta*, established between 1980 and 2005, with an approximate density of 700-900 trees ha^{-1} (Mendez-Casariego et al., 2005). At present, some plantation patches are affected by the woodwasp *Sirex noctilio* (Hymenoptera: Siricidae; Mendez-Casariego et al., 2005).

2.2. Experimental design

The study workflow comprises four main components: (1) land cover classification to identify native forest and pine plantations; (2) field sampling for AGB and biodiversity data collection; (3) estimation and mapping of regional AGB carbon stocks including associated uncertainty, using field data and remote sensing imagery; and (4) analysis of the spatial distribution of AGB carbon stock in relation to topographic variables and vegetation (Fig. 2).

2.2.1. Land cover classification

We used Sentinel-2 multispectral surface reflectance imagery to construct cloud-free mosaics between January 2023 and December 2024, applying snow and shadows masks. Most spectral bands from this satellite constellation were used, along with vegetation indices (Table S3a and b) and an elevation band (digital elevation model from the USGS, USA). The study used 70% of the data points for training and 30% for validation, incorporating data from both field sampling and high-resolution imagery (Google Earth®). The mosaics were classified using Random Forest supervised classification into seven distinct classes based on the training data: native forests, pine plantations, native shrub steppe, native grass steppe, wetlands, bare soil, and water (Fig. 1B). Only native forests and pine plantations were retained for subsequent analysis after mask application.

2.2.2. Field sampling for aboveground biomass (AGB) and biodiversity data collection

We surveyed field plots in December 2023 and 2024 following the VCS (Module VMD 0001, 2013) protocols for AGB carbon estimation. We randomly established forty 20 × 20 m plots −20 in native forests and

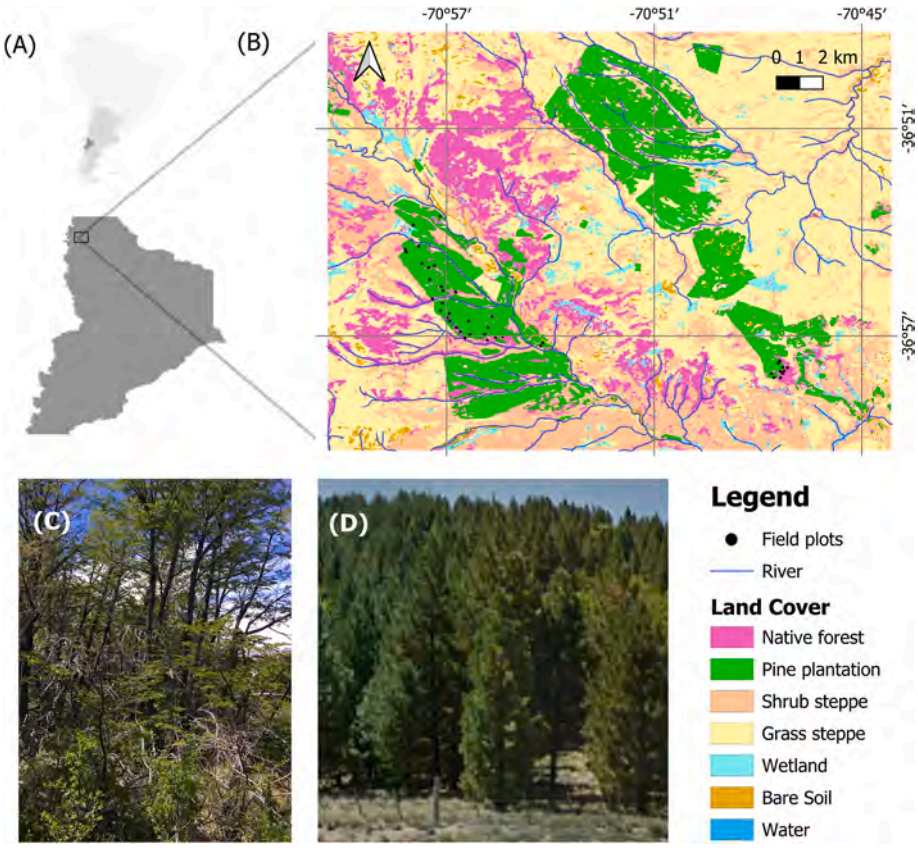

Fig. 1. (A) Study area located in the northwest Patagonia mountains, Neuquén province, Argentina. (B) Supervised classification map of land cover: native forest, pine plantations, shrub steppe, grass steppe, wetlands, water, and bare soil. The black points represent the sample plots. Field photos showing: (C) native forest and (D) pine plantations (PH, Google Earth®). Projection: UTM 19S (analysis), WGS84 (display).

20 in pine plantations (Fig. 1C and D)—and georeferenced them using a handheld GPS (Garmin eTrex 30®). The plots span an elevational range of 1300-1700 m a.s.l. In each plot, all woody individuals with a stem diameter at breast height (DBH, at 1.3 m) > 5 cm were recorded, with measurements of DBH (cm), total height (H, m), and crown diameter (CD). Shrubs (multi-stemmed woody plants) and small trees (single-stemmed individuals with DBH <5 cm) were sampled within four randomly placed 5 × 5 m subplots. Herbs were also measured in the subplots for biodiversity record but were not considered for AGB calculations. For shrubs and small trees individuals, we measured height and the longest and perpendicular crown diameters. We calculated the mean crown diameter (CD) as the average of the two measurements: $CD = (D_1 + D_2)/2$. We used a tape to measure stem and crown diameter and a hypsometer (Nikon Forest®) for tree height. We taxonomically identified each individual to the species or genus level, and recorded its growth form and status (endemic, native, non-native) using the online database of the Instituto de Botánica Darwinion, IBODA, 2025 (http://www.darwin.edu.ar/) (Table S1).

We estimated aboveground dry biomass (AGB) using species-specific allometric equations (Table S2). Within plots (for trees) or subplots (for shrubs), we summed all individual AGB measurements to obtain total AGB per hectare. Finally, we calculated carbon stock by multiplying the dry AGB by a carbon coefficient of 0.47 (IPCC et al., 2006).

For each field plot, we calculated forest structural variables, aboveground dry biomass (AGB), and AGB carbon stock. Additionally, we calculated understory species richness, and cover (shrub, subshrubs and herbaceous vegetation) by aggregating values at the subplot level. We compared these variables among vegetation types using the nonparametric Wilcoxon test for independent samples.

2.2.3. Estimation and mapping of regional AGB carbon using multisensor satellite imagery

We estimated landscape-level AGB carbon stocks using a single Random Forest regression model (Breiman, 2001), jointly fitted to native forests and pine plantations, within a Nested Cross-Validation (Nested CV) framework (Vabalas et al., 2019; Larracy et al., 2021). Field plot–derived AGB carbon stocks served as ground truth. Predictors included remote-sensing variables (Sentinel-2, Sentinel-1, GEDI, and Copernicus DEM GLO-30) and vegetation type, recorded in the field as a categorical variable.

All raster layers and vector ROIs (field plots) were reprojected to a 10 m spatial resolution and matched to a common CRS (WGS 84/UTM zone 19S). Spatial overlap was verified before extraction to ensure geometric consistency. Remote sensing processes were conducted using the Google Earth Engine® platform. All spatial analyses were performed in UTM 19S projection (EPSG:32719). Maps were displayed via on-the-fly reprojection, and geographic coordinates (WGS 84, EPSG:4326) were shown for reference.

2.2.3.1. Remote sensing source and data processing. A collection of the Sentinel-2 Multi-Spectral Instrument Level 2A surface reflectance products (10 m spatial resolution) was acquired for the period 2023-2024, selecting images with a cloud density below 5%, and applying masks for water, snow, and shadows. We used single spectral bands, along with the vegetation index (Table S3a and b), and computed median monthly values for the two years.

C-band Synthetic Aperture Radar (SAR) imagery from the Sentinel-1A/B satellites (10 m spatial resolution) was obtained for the same period. We preprocessed the scenes using radiometric calibration, terrain correction using the 30 m Copernicus DEM GLO-30, and a Speckle noise filter (focal median with a radius of 15 m; Moreira et al.,

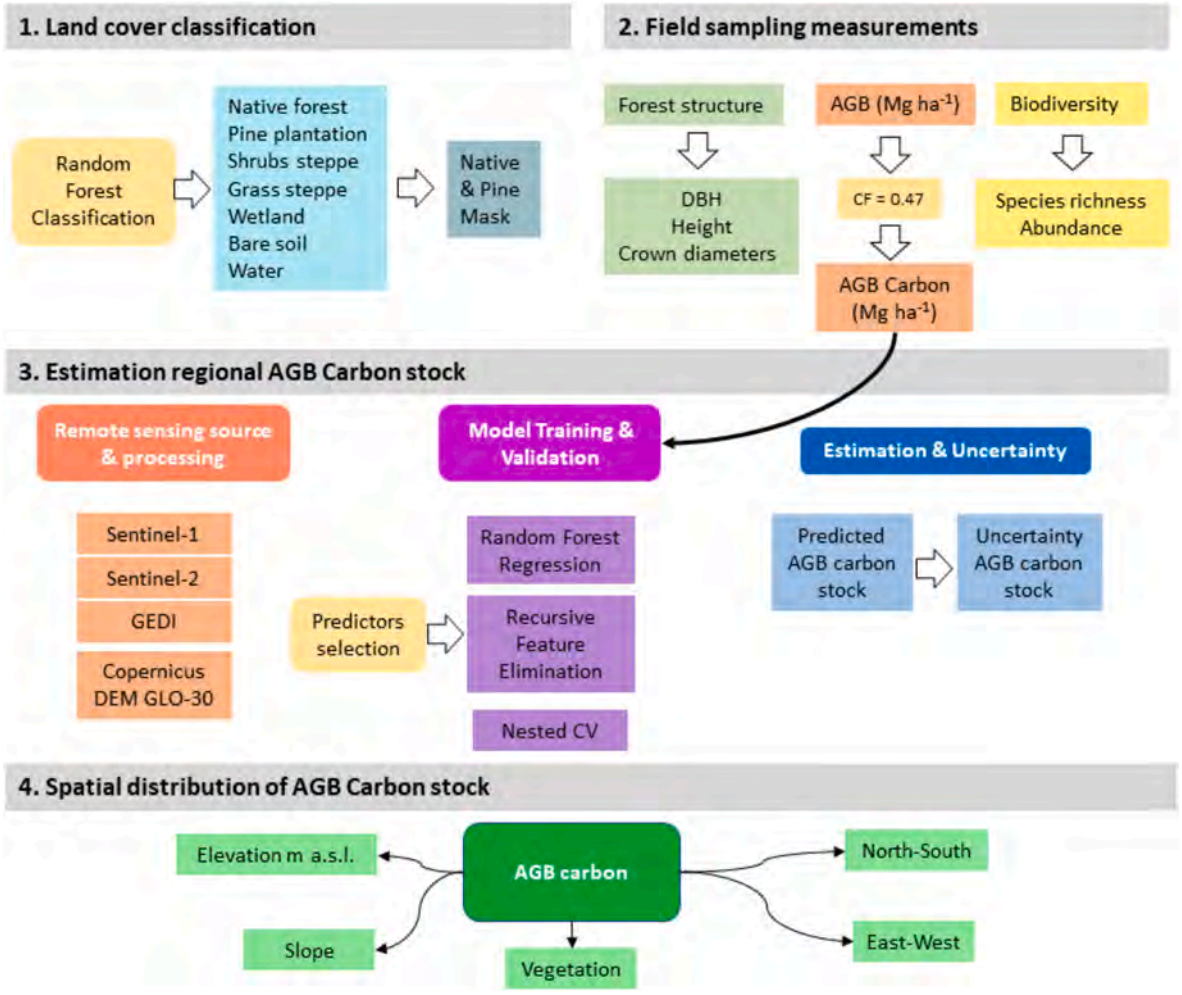

Fig. 2. Study workflow: (1) land cover classification. (2) field sampling for AGB and biodiversity data collection, followed by AGB to-carbon conversion; (3) estimation and mapping of regional AGB carbon stocks using field data and remote sensing imagery, based on Random Forest regression with Recursive Feature Elimination, with model performance and validation evaluated through Nested Cross Validation (R^2, *RMSE*, *RMSE*%); and (4) analysis of the spatial distribution of AGB carbon stock in relation to topographic variables (elevation, slope, aspect) and vegetation type (native forest and pine plantations). Final outputs include forest structure, biodiversity metrics, and predicted AGB carbon stock with associated uncertainty map.

2013). The ground range detected high-resolution products (GRD), acquired in the Interferometric Wide (IW) swath mode, were considered. We used the backscatter dual polarizations VV (vertical-vertical) and VH (vertical-horizontal) in ascending and descending orbit pass direction, for which we calculated the temporal mean (Table S3a). From the backscatter coefficients, we derived three SAR-based indices: (a) the VV/VH cross polarization ratio, which represents the relation among dense and sparse vegetation (Dong et al., 2024); (b) the Radar Vegetation Index (RVI), an indicator of vegetation quantity and structure (Holtgrave et al., 2020); and (c) superficial soil moisture index (SSM), computed for ascending and descending orbits of VV polarization data (Bauer-Marschallinger et al., 2018).

The Global Ecosystem Dynamics Investigation (GEDI) mission is a full-waveform LiDAR instrument designed to collect samples of the forest vertical structure with eight 25 m footprints, spaced approximately 60 m apart (Dubayah et al., 2020). We used the V2.1 version of the GEDI-L2A Monthly dataset, for which we considered the canopy height (rh98), corresponding to the relative height metrics at 98% of energy return relative to the ground (Table S3a). We filtered the GEDI shots to obtain high-quality footprints, selecting degradation = 0, quality flags = 1, sensitivity >0.95, night shots, and terrain slope <30° following Adrah et al. (2025). Due to the limited number and sparse distribution of GEDI footprints (Dubayah et al., 2020), we included datasets collected between 2022 and 2024 to increase spatial coverage. Filtered GEDI-L2A canopy height data were integrated with pre-processed Sentinel-2 imagery and topographic variables from Copernicus GLO-30 (elevation, slope, and aspect), to generate a continuous wall-to-wall, high-resolution map using Random Forest regression (Dong et al., 2024). This approach allowed the spatial extrapolation of GEDI-derived structural metrics to areas not directly sampled by the sensor. The target variable (rh98) and predictor layers were spatially aligned to a common 10 m grid, and spatial aggregation was performed using mean reduction. We extracted 100 training samples from pixels with valid GEDI data after filtering and randomly split them into training (70%) and testing (30%) subsets. The resulting raster layer, with an R^2 of 0.75 and an *RMSE of* 33.63%, was used as a predictor variable in subsequent modelling analyses.

Topographic variables (elevation, slope and aspect) were extracted from the Copernicus DEM GLO-30 and incorporated as predictors into the AGB carbon model (Table S3a). The aspect variable was converted to radians and calculated the sine and cosine of this angle to obtain the lineal east-west and north-south variables.

2.2.3.2. Model training and validation. AGB carbon stock was estimated using Random Forest regression and the Nested CV algorithm in R (R Core Team, 2025) with *nestcv* package (Table S4). Feature selection was

performed using the Recursive Feature Elimination (RFE) algorithm (Gregorutti et al., 2017) which identifies the minimal set of predictors that maximizes predictive performance while reducing model complexity. Root Mean Square Error (*RMSE*) was used as the optimization metric. The hyperparameters for the Random Forest model were optimized via a grid search over the number of trees (50–1700) and the number of variables per split (1–4) (Breiman et al., 2018). Variable importance was derived from the model's internal out-of-bag (OOB) error estimates.

To avoid pseudoreplication and ensure spatial correspondence between field data and satellite predictors, remote-sensing variables were aggregated at the plot level (20 × 20 m) using an area-weighted mean based on the effective intersection area of pixels. This procedure ensures that each plot contributes a single representative predictor vector for the sampled area.

We evaluated the performance of the Random Forest regression model using five-fold Nested CV, stratified by vegetation type to ensure balanced representation of both forest types in each fold. Nested CV consists in two hierarchical loops that ensure a strict separation between the dataset for model training and final model validation. In the outer loop, the dataset is partitioned into five equal folds, of 8 plots each. During each of the five iterations, 20% of the data (one fold, 8 plots) is set aside exclusively for validation, while the remaining 80% (four folds, 32 plots) is used for the model development phase. The inner loop operates within that 80% of the data, and is dedicated to development steps, specifically feature selection and hyperparameter tuning. By isolating these processes to the inner loop, the methodology prevents "information leakage," ensuring that the final test data remains entirely "unseen" during the optimization of the model. Once the model is fully refined in the inner loop, its performance is measured using the 20% validation fold that was initially held out. This entire procedure is repeated five times, rotating the validation set in each turn so that every data point is eventually used for testing but never for the development of the specific model that evaluates it. Model performance was quantified using the coefficient of determination (R^2), root mean square error *(RMSE*), relative *RMSE (RMSE%*), mean absolute error (*MAE*), and Bias. Final performance metrics were obtained by averaging these values across the five outer folds. This nested approach is crucial because it provides an unbiased and robust estimate of how the model will perform on new datasets, especially when working with limited sample sizes (Vabalas et al., 2019; Larracy et al., 2021).

2.2.3.3. Model uncertainty. We developed the uncertainty map of AGB carbon stock predictions following the procedure by Silveira et al. (2023). Specifically, we grouped the predicted AGB carbon stock values into 5 bins and calculated the *RMSE%* for each bin. We then fitted a polynomial regression model to the binned *RMSE%* values as a function of the mean predicted AGB carbon stock. Finally, we mapped the spatial distribution of *RMSE%* uncertainty and compared uncertainty patterns across vegetation types, elevations, slopes, and aspects.

2.2.4. Comparison with global AGB carbon model

Finally, we compared our modelled AGB carbon stocks with estimates from GEDI Level 4A (L4A) products (Dubayah et al., 2022). We used GEDI Version 2.1 aboveground biomass density (AGBD, Mg ha^{-1}), converting biomass to carbon stock by multiplying by 0.47 (IPCC et al., 2006). Model agreement was evaluated via cross-validation (R^2) and *RMSE (%*) and Pearson's correlation coefficient (r).

2.2.5. Spatial distribution of AGB carbon stock

We analyzed the spatial distribution of aboveground biomass (AGB) carbon stock in relation to topography using three complementary approaches. First, we explored the relationship between predicted AGB carbon stock (from the Random Forest model), topographic variables (elevation, slope, north–south and east–west components), and vegetation type through graphical analyses of spatial outputs, primarily for interpretability. Second, to improve model interpretability beyond prediction, we applied post-hoc analyses following Simon et al. (2023). We assessed non-linear effects and interactions among the predictors retained in the final Random Forest regression on the predicted AGB carbon stock. We used partial dependence plots (PDPs), local predictors slope estimates across elevation quantiles, and the Friedman H-statistic. These analyses were implemented using the *pdp* and *iml* packages (Table S4) in R. Third, we evaluated the relationship between observed AGB carbon stock and topographic variables using Generalized Additive Models (GAMs) with a Gaussian error distribution. The response variable was log-transformed, and continuous predictors were standardized. Vegetation type was included as a categorical factor, and smooth terms were fitted using thin plate regression splines with restricted basis dimensions. Model selection was based on Akaike Information Criterion (AIC), diagnostic checks, and parsimony. Analyses were conducted using the *mgcv* package in R (Table S4).

3. Results

3.1. Land cover classification

The land cover classification (Fig. 1B) revealed that native grass steppe vegetation dominated the landscape (42%, 22,566 ha), followed by native shrub steppe (24%, 12,908 ha), pine plantations (15%, 8056 ha), native forest (14%, 7540 ha), wetlands (3%, 1702 ha), and bare soils (2%, 974 ha). The Random Forest out-of-bag (OOB) accuracy was 85%, with a Kappa Index of 0.81, indicating good classification performance.

3.2. Field-based AGB and biodiversity measurement

Field measurements showed marked structural and biodiversity differences between native forests and pine plantations (Table 1). Total AGB was 80% higher in pine plantations than in native forests, consistent with the significantly larger tree size in plantations, both in DBH and height. Tree density did not differ significantly between vegetation types. In contrast, native forests showed significantly higher shrub and subshrub densities than plantations. Moreover, native forest plots exhibited significantly greater understory vegetation cover (%) and species richness than pine plantations, with percentage differences of 190% and 195%, respectively (Table 1; Table S1).

3.3. Estimation and mapping of regional AGB carbon stock using multisensor satellite imagery

3.3.1. Variable selection and model performance

Modelling AGB carbon across the northwestern Patagonian mountains using our field data and selected remote-sensing predictors resulted in moderate model performance (Fig. 3a). The coefficient of variation (CV) of the performance metrics across the five folds ranged from 12.5% for R^2 to 31% for *RMSE%*. The computed out-of-bag (*OOB*) error was 22.98 Mg C ha^{-1}, consistent with the *RMSE* validation metric (Table 2). The RFE process identified an optimal set of seven predictor variables in descending order of importance (Fig. 3b): B5 (Red Edge 1 band), superficial soil moisture index (SSM), enhanced vegetation index (EVI), VV/VH, B11 (SWIR 1), B4 (red), and DEM (elevation). The optimal hyperparameter configuration used 100 trees and 2 *mtry*.

The predicted AGB carbon stock ranged between 10 and 136 Mg C ha^{-1}, with a mean value of 46 Mg C ha^{-1}, corresponding 25.20 ± 0.02 (SE) for native forest and 64.30 ± 0.70 (SE) Mg C ha^{-1} for pine plantations, respectively (Fig. S3). The 75% of AGB carbon density distribution in native forests was concentrated around 13 to 30 Mg C ha^{-1}, with a small number of patches of high AGB carbon stock (between 50 and 100 Mg C ha^{-1}). In contrast, 75% of the AGB carbon stock density distribution in pine plantation was more homogeneous, ranging

Table 1
Structural characteristics and biodiversity metrics of native forests and pine plantations in the northwestern Patagonian mountain region, Argentina. Values represent mean ± SE, and the number of plots (n) is indicated for each metric. Statistical comparisons were performed using Wilcoxon tests. Significant differences ($p < 0.05$) are shown in bold. Density values (ind. ha^{-1}) are presented separately for trees, shrubs, and subshrubs. DBH (cm) and height (m) correspond to mean values for trees and shrubs. Understory cover (%) and species richness refer to shrubs, subshrubs, and herbaceous species.

Metric	Native forest (mean ± SE)	Pine plantation (mean ± SE)	Test	p
Total AGB (Mg ha^{-1})	81.93 ± 18.24 (20)	190.36 ± 18.75 (20)	**W = 70**	**<0.0001**
C stock (Mg C ha^{-1})	38.51 ± 8.57 (20)	89.47 ± 8.81 (20)	**W = 60**	**<0.001**
Tree Density (Ind ha^{-1})	1157.5 ± 324.41 (20)	1047.30 ± 88.90 (20)	W = 159	0.27
Shrubs Density (Ind ha^{-1})	1340 ± 249.78 (20)	0.0 ± 0.0 (20)	**W = 370**	**<0.001**
Subshrubs Density (Ind ha^{-1})	3730 ± 561.02 (20)	60 ± 50.47 (20)	**W = 399**	**<0.0001**
DBH (cm)	8.311 ± 1.12 (20)	29.48 ± 1.50 (20)	**W = 3**	**<0.0001**
Height (m)	2.79 ± 0.29 (20)	15.93 ± 0.81 (20)	**W = 0**	**<0.0001**
Understory cover%	56.49 ± 9.15 (20)	0.44 ± 0.30 (20)	**W = 396**	**<0.0001**
Understory Richness (S)	4.60 ± 0.34 (20)	0.15 ± 0.10 (20)	**W = 399**	**<0.0001**

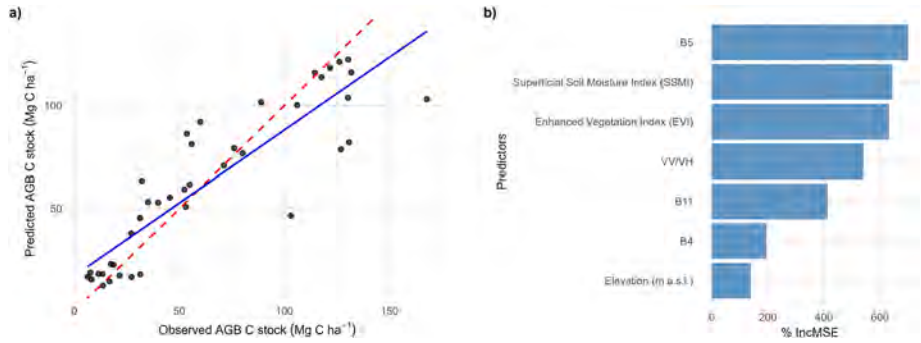

Fig. 3. a) Predicted vs. observed values of aboveground biomass (AGB) carbon stock (Mg C ha^{-1}) model. Points represent the validation dataset (unseen data) of five folds Nested CV in Random Forest regression. The blue line represents the fitted relationship, and the red line represents the 1:1 line. b) Relative importance of the selected model predictor variables (% IncMSE). (For interpretation of the references to colour in this figure legend, the reader is referred to the Web version of this article.)

Table 2
Model performance metrics using the selected predictor variables for AGB carbon stock (Mg C ha^{-1}). Values for R^2, *RMSE, RMSE%,* and *MAE* represent the mean nested cross-validation (CV) estimates from the Random Forest Regression model on unseen data. Values in parentheses indicate the minimum and maximum across the five nested cross-validation folds.

Metric	Mean (min - max)
R^2	0.78 (0.65-0.88)
RMSE (Mg C ha^{-1}*)*	21.67 (13.85-28.29)
RMSE%	33.86 (24.18-49.57)
MAE (Mg C ha^{-1}*)*	14.78 (10.76-20.99)
Bias (Mg C ha^{-1}*)*	1.38 (−7.81-5.43)

between 55 and 78 Mg C ha^{-1} (Fig. S3) and extending up to 133 Mg C ha^{-1}. The total AGB carbon stock of this region was estimated at approximately 696 and 1950 Gg CO_2 equivalents (converted from carbon stock using a factor of 44/12) in native forest and pine plantations, respectively. While native forest and pine plantations occupied similar proportions of the landscape (48% and 52%, respectively), their contributions to total AGB carbon stocks differed: native forests accounted for 26%, whereas pine plantations contributed 74%.

3.3.2. AGB carbon map

The AGB carbon map predicted by our model revealed a heterogeneous spatial distribution across the study area, with elevation acting as a potential important environmental driver (Fig. 4). Higher predicted AGB carbon values were concentrated in the southwestern portion of the study area, which coincided with mid elevations, flat slopes, and pine plantation stands. Lower and spatially sparse AGB carbon values were more frequent in the eastern region, corresponding to sites with higher elevation and steeper slopes, largely associated with native forest. However, these results should be interpreted cautiously, as they extend beyond the range of the training data. As expected, pine plantations exhibited higher AGB carbon than native forests.

3.3.3. Model uncertainty

The relationship between the relative uncertainty (RMSE%) and predicted AGB carbon stock, showed a good fit (R^2 = 0.85, RMSE = 2.96%). At low to intermediate predicted AGB carbon levels, relative uncertainty was high (48%). As predicted AGB carbon increased, uncertainty decreased, reaching values below 10% at the highest carbon levels (Fig. S1). Model uncertainty also varies across vegetation types. Native forests showed higher RMSE% values with a more concentrated distribution, whereas pine plantations exhibited greater dispersion, with values ranging from very low to very high uncertainty (Fig. S2). The spatial distribution of relative RMSE% suggests a potential increase in prediction uncertainty with elevation, particularly for pine plantations, while for native forest it remained relatively constant along the gradient (Fig. S2a). Slope and aspect (north-south and east-west) exhibited weaker and flatter relationships with uncertainty (Fig. S2b–d).

3.3.4. Comparison with global AGB carbon model

The comparison between predictions from our AGB carbon model and those from the model developed by GEDI L4A showed good Pearson correlation (r = 0.86; $p < 0.001$), and moderate to low agreement (R^2 = 0.73 and *RMSE* = 29.61 Mg C ha^{-1}; *RMSE* = 66.34% Fig. S3). This discrepancy could be related, among other factors, to a geolocation issue affecting GEDI LiDAR shots (Adrah et al., 2025).

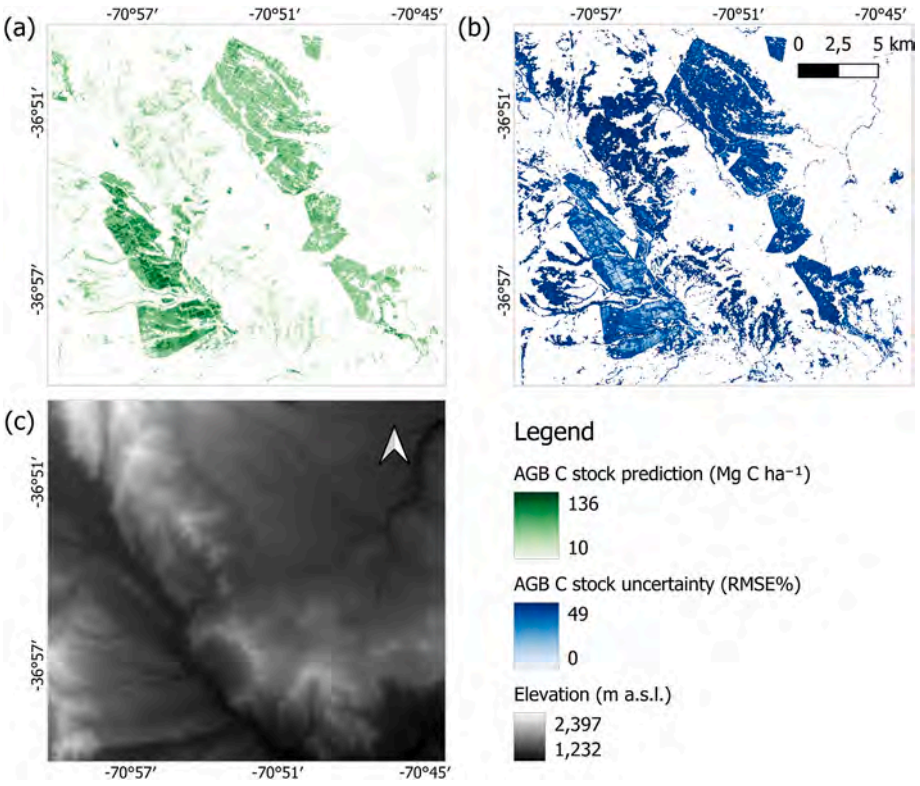

Fig. 4. Spatial patterns of aboveground biomass (AGB) carbon stock (Mg C ha^{-1}) across the northwestern Patagonia mountains: a) predicted values, b) model uncertainty, expressed as relative *RMSE (%),* and c) elevation map (m a.s.l.). White areas represent grass and shrub steppe, wetlands, and bare soil covers, which were masked prior to modelling. All analyses were performed in the UTM projection (EPSG:32719), and geographic coordinates are expressed in WGS 84 (EPSG:4326).

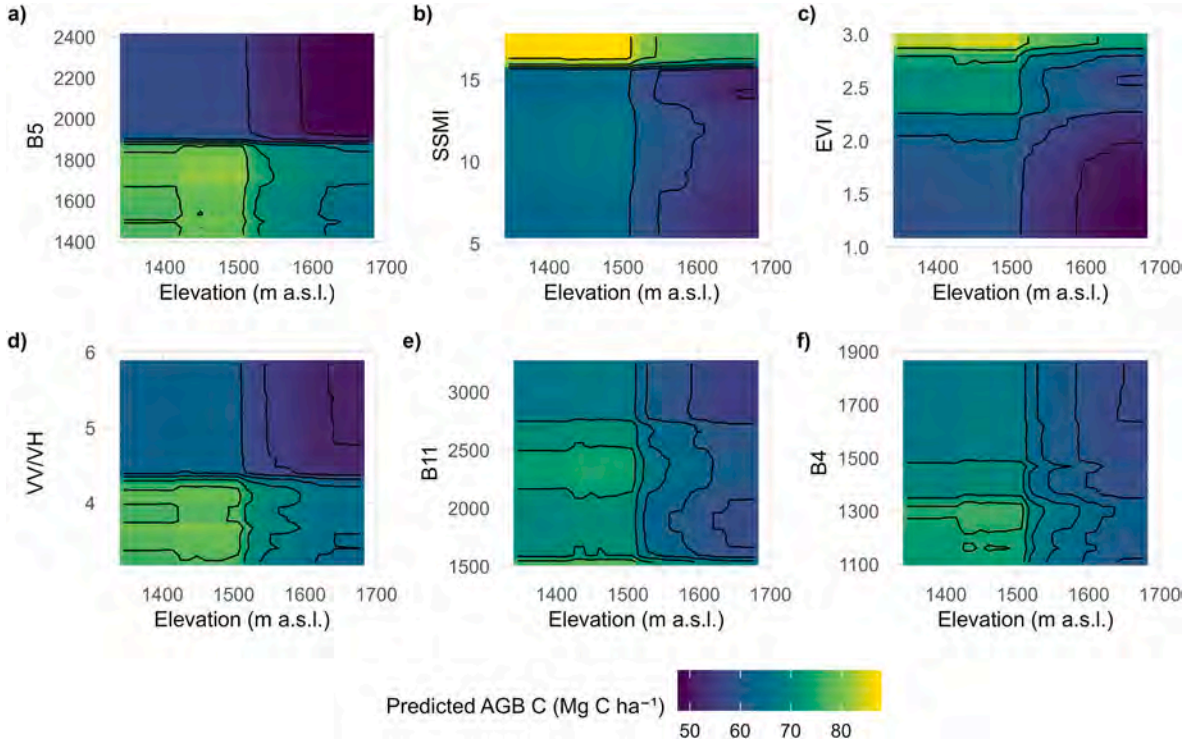

Fig. 5. Two-dimensional partial dependence plots illustrating the joint effects of elevation (DEM) and selected spectral and radar predictors on predicted aboveground biomass carbon (AGB C stock, Mg C ha^{-1}) from the Random Forest model. Panels show interactions between DEM and (a) B5, (b) superficial soil moisture index (SSMI), (c) enhanced vegetation index (EVI), (d) VV/VH ratio, (e) B11, and (f) B4. Color gradients represent predicted AGB C stock, while contour lines indicate response surfaces. Non-parallel contour patterns suggest interactions between predictors. All other variables were held constant at their observed values during partial dependence estimation. (For interpretation of the references to colour in this figure legend, the reader is referred to the Web version of this article.)

3.4. Spatial distribution of AGB carbon stock

The first approach of graphics of predicted AGB carbon from Random Forest, in both forest types exhibited a unimodal relationship with elevation, which was more pronounced in pine plantations. Maximum predicted values occurred at mid-elevations (1400–1500 m a.s.l.), followed by a decline at both higher and lower elevations. No pine stands were recorded above 1800 m a.s.l., whereas native forests showed a weak, negative trend across the upper elevational range (Fig. S4a). Predicted AGB carbon decreased slightly with increasing slope in both vegetation types (Fig. S4b). In contrast, the north–south and east–west topographic components had negligible influence on predicted AGB carbon (Fig. S4c and d).

The second approach showed that Elevation (DEM) exerted a strong negative effect on predicted AGB carbon stock across all partial dependence analyses (Fig. 5), indicating a consistent topographic constraint on AGB carbon stock. The relationship between AGB carbon and remotely sensed predictors—used here as proxies of vegetation structure—varied along the elevation gradient. The positive effect of EVI weakened with increasing elevation (slope curve: 12.9 to 11.4–11.7; Fig. 5c; Table S5), while the negative effect of VV/VH ratio became less pronounced (slope curve: −8.82 to −7.76; Fig. 5d; Table S5). Spectral bands (B5, B11, B4) showed weak negative relationships with AGB, with minor attenuation at higher elevations (Fig. 5a–e and f; Table S5), whereas soil moisture maintained a relatively stable positive effect (slope curve:1.4; Fig. 5b; Table S5) across the DEM gradient.

Interaction strength between Random Forest predictors, quantified using the Friedman H-statistic, were generally low to moderate (Table S6). Elevation showed modest interaction effects (H = 0.07), indicating that its influence on AGB carbon stock is largely additive but still modulates the relationship with the other predictors. The strongest pairwise interactions with DEM were observed for B4 and VV/VH ratio, although effect sizes remained limited.

The third approach showed that GAM explained a high proportion of the variability in observed AGB C stock (adjusted $R^2 = 0.74$; deviance explained = 78.1%), indicating a good model fit given the limited sample size (n = 40). Pine plantations had significantly higher AGB C than native forests ($\beta = 1.03 \pm 0.16$; $p < 0.001$). Elevation exhibited a non-linear effect on AGB C stock in both vegetation types (Fig. 6a), although its statistical significance differed between them. In native forests, this relationship was significant (edf = 2.43; p = 0.003), showing a decline in AGB C at higher elevations, whereas in pine plantations the non-linear trend was weaker and not statistically significant (edf = 2.12; p = 0.13). Slope showed a significant negative effect across vegetation types ($\beta = -0.316 \pm 0.088$; p = 0.001), with AGB C decreasing monotonically with increasing slope (Fig. 6b).

4. Discussion

Our results indicate that topography—particularly elevation—even across relatively small gradients, plays a central role in structuring the spatial distribution of AGB carbon stocks in both forest types. Although pine plantations showed high AGB carbon storage, native forests reached comparable values under specific topographic conditions and remain critical for the conservation of endemic biodiversity in semiarid mountain landscapes, highlighting a trade-off between carbon storage and biodiversity conservation.

The observed east–west increase in AGB carbon stocks (Fig. 4a) aligns with the regional precipitation gradient described for Patagonia (Paruelo et al., 1998), but also reflects the spatial concentration of older pine plantations (pers. obs.) and high-biomass native forest patches at mid-elevations and on gentle slopes. Such topographic positions are relatively limited in mountain environments and are typically characterized by higher soil fertility, greater soil depth, and enhanced water retention due to sediment accumulation (Bran et al., 2002). These conditions may promote greater allocation of plant resources to the aboveground biomass, resulting in higher carbon stocks (Zhao et al., 2023). Moreover, their accessibility facilitates forest management. Together, these characteristics likely explain both the preferential establishment of pine plantations and the relatively high structural development observed in native forests at these locations.

Native forests were distributed across a broader range of elevation and slope, including sites where reduced pine growth and AGB carbon accumulation would also be expected. In this semiarid region, *N. antarctica* frequently forms shrubby thickets composed of small, multi-stemmed individuals; but it can develop a tree-like physiognomy under more favorable moisture conditions (Ramírez et al., 1985; Steinke et al., 2008). Consistent with this plasticity, our data show marked differences in AGB carbon stocks between shrub-dominated stands (7–20 Mg C ha^{-1}) and tree-form patches (27–130 Mg C ha^{-1}). Despite this limitation, our results align with Reiter et al. (2025), showing that *N. antarctica* can reach AGB carbon stocks comparable to *P. ponderosa* in optimal topographic settings that favor its tree-form development. These findings underscore the importance of conserving and restoring native forests in sites that promote their full structural development.

Native forests consistently supported higher species richness than pine plantations, likely reflecting their greater structural complexity and vertical stratification, which enhance niche availability and species coexistence (Brockerhoff et al., 2008). Pine plantations, in turn, tend to reduce biodiversity due to management-related factors such as understory removal, limited regeneration opportunities under closed canopies, and alterations in soil properties (Brockerhoff et al., 2008; Simberloff et al., 2010; Hua et al., 2022). Therefore, forest management approaches should recognize that multifunctional landscapes require a balance among carbon storage, biodiversity conservation, and long-term

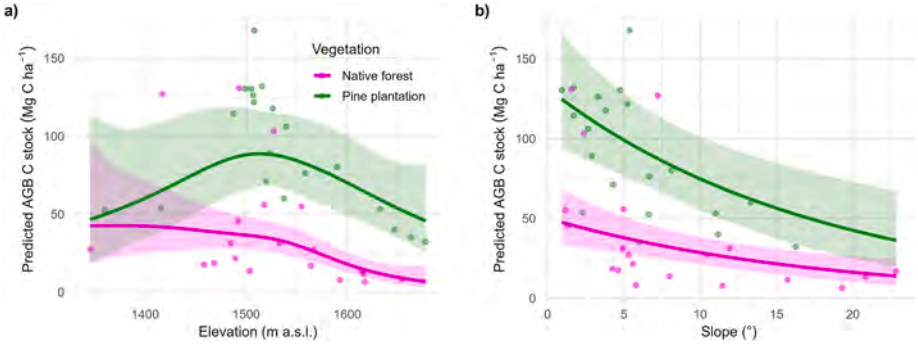

Fig. 6. Effects of topographic variables on observed aboveground biomass carbon (AGB C stock) derived from the Generalized Additive Model (GAM). (a) Partial effect of elevation (DEM) on AGB C stock, showing vegetation-specific non-linear responses for native forest and pine plantations. (b) Effect of slope on AGB C stock, illustrating a consistent monotonic decrease across vegetation types. Solid lines represent model predictions and shaded areas indicate 95% confidence intervals. Points correspond to observed values. All predictions were back-transformed from the log scale.

ecosystem resilience.

4.1. Study scope and limitations

The land-cover classification (Fig. 1B) showed sufficient accuracy to distinguish native forest from pine plantation, enabling reliable model application. The estimated mean AGB carbon stock of native forests and pine plantations fell within the range reported for the region (Laclau, 2003; Araujo and Austin, 2020), and was lower than values documented in more humid *N. antarctica* forests of southern Patagonia (Peri et al., 2010; Loguercio et al., 2024), likely reflecting climatic differences.

The model produced a high-resolution AGB carbon stock map with moderate-to-good predictive performance and associated uncertainty, capturing spatial patterns primarily related to vegetation type and elevation. Model accuracy (Table 2) was comparable to studies employing similar methodological approaches and field sample sizes, such as Xu et al. (2023) in temperate forests of China, and exceeded that reported for subtropical forests in Argentina (Gasparri and Baldi, 2013). SAR and optical imagery were the most influential predictors. The superficial soil moisture index (SSM) should be interpreted with caution in mountainous and forested systems, as it may capture canopy moisture or structure rather than actual soil moisture (Bauer-Marschallinger et al., 2018). Consistent with Pötzschner et al. (2022), the inclusion of GEDI-LiDAR canopy height metric did not improve model performance, possibly due to geolocation uncertainty in GEDI footprints (Adrah et al., 2025).

The decrease in uncertainty (*RMSE%)* with increasing values of predicted AGB carbon stock is consistent with Silveira et al. (2023), likely reflecting an improved signal-to-noise ratio in structurally developed stands. In line with our results, Silveira et al. (2023) also showed greater uncertainty in forests dominated by smaller trees, with lower uncertainty observed in flat terrain and gentle slopes. Differences in uncertainty between vegetation types suggest that plantations, although sometimes structurally homogeneous, can display considerable spatial heterogeneity related to stand age, density, management practices, and canopy condition. Accordingly, predicted AGB carbon values at the lower end of the distribution should be interpreted with caution, as they are associated with comparatively higher relative uncertainty.

Future work would benefit from a larger number of field plots spanning broader topographic gradients (elevation, slope, aspect). Developing vegetation-specific models may further improve performance, as different forest types can exhibit distinct relationships with remote sensing predictors (Holtgrave et al., 2020). Incorporating additional carbon pools—such as soil organic and inorganic carbon, litter, and dead wood—would provide a more comprehensive assessment of total ecosystem carbon stocks (Körner, 2017; Pan et al., 2024). Although topographic variables were included to capture environmental heterogeneity, they act as indirect proxies for underlying drivers such as soil properties, water availability, and climatic conditions. As a result, the observed relationships between topography and AGB carbon should be interpreted as correlative rather than mechanistic, and the relative contribution of specific environmental factors cannot be disentangled within the current framework. Finally, the influence of disturbance regimes, stand age, and edaphic factors should also be evaluated to further refine landscape-scale carbon estimates.

4.2. Forest management and conservation

Within the framework of nature-based climate solutions, our results suggest that forest management strategies in semiarid mountain regions should move beyond carbon-centric approaches in order to explicitly integrate topography, vegetation type, and biodiversity considerations. From a spatial planning perspective, mid-elevation zones (1400–1500 m a.s.l.) and gentle slopes (0-10°) where native forests concentrate their highest AGB carbon stocks, should be considered high-priority areas for conservation and restoration (Griscom et al., 2017; Körner, 2017; Ameray et al., 2021). These topographic sites are spatially limited and often overlap with suitable areas for pine plantations, indicating that the expansion of carbon-oriented forestry in these zones may entail biodiversity losses, including endemic species In this context, avoiding further conversion of native forests, particularly in key topographic positions, could help maintain multifunctional landscapes and reduce trade-offs between carbon storage and biodiversity conservation (Hua et al., 2022).

5. Conclusions

We found that in semi-arid mountain environments, the widespread assumption that exotic plantations necessarily store more carbon than native forests does not consistently hold true. Our results indicate that, under specific topographic conditions—particularly at mid-elevations and on gentle slopes—native forests can approach comparable AGB carbon stocks to those of pine plantations. Moreover, the higher levels of biodiversity, particularly endemism, recorded in native forests underscore their importance for conservation and restoration strategies. Together, these findings emphasize the need to account for local topographic context when assessing carbon storage potential across forest types, and to integrate biodiversity considerations to ensure full ecosystem functioning. Such an integrated perspective is particularly relevant for international crediting frameworks that aim to incorporate both carbon storage and biodiversity within broader ecosystem conservation objectives.

CRediT authorship contribution statement

Tatiana Alejandra Valfré-Giorello: Conceptualization, Data curation, Formal analysis, Investigation, Methodology, Software, Validation, Writing – original draft, Writing – review & editing. **Lisandro Agost:** Formal analysis, Methodology, Software, Visualization, Writing – review & editing. **Georgina Conti:** Conceptualization, Investigation, Supervision, Writing – review & editing. **Carla Montero:** Conceptualization, Funding acquisition, Project administration, Resources, Supervision, Writing – review & editing. **Maria Elena Oneto:** Conceptualization, Funding acquisition, Project administration, Resources, Supervision, Writing – review & editing. **Daniel Roberto Pérez:** Conceptualization, Funding acquisition, Investigation, Project administration, Resources, Supervision, Validation, Writing – review & editing.

Declaration of competing interest

The authors declare that they have no known competing financial interests or personal relationships that could have appeared to influence the work reported in this paper.

Acknowledgements

This study is part of the Post-Doctoral research of T.A. Valfré-Giorello, with a scholarship from CONICET and Y-TEC, Argentina. Funding was provided by Y-TEC through FUNYDER. We are grateful to Dr. R.C. Torres, Lic. J. Hernández, and Lic. F.N. Zorbalas for their support during fieldwork.

Appendix A. Supplementary data

Supplementary data to this article can be found online at https://doi.org/10.1016/j.jaridenv.2026.105651.

Data availability

The data that has been used is confidential.

References

Adrah, E., Wong, J.P., Yin, H., 2025. Integrating GEDI, Sentinel-2, and Sentinel-1 imagery for tree crops mapping. Rem. Sens. Environ. 319, 114644. https://doi.org/10.1016/j.rse.2025.114644.

Ameray, A., Bergeron, Y., Valeria, O., Montoro Girona, M., Cavard, X., 2021. Forest carbon management: a review of silvicultural practices and management strategies across boreal, temperate and tropical forests. Current Forestry Reports 1–22. https://doi.org/10.1007/s40725-021-00151-w.

Araujo, P.I., Austin, A.T., 2020. Exotic pine forestation shifts carbon accumulation to litter detritus and wood along a broad precipitation gradient in Patagonia, Argentina. For. Ecol. Manag. 460, 117902. https://doi.org/10.1016/j.foreco.2020.117902.

Bauer-Marschallinger, B., Freeman, V., Cao, S., Paulik, C., Schaufler, S., Stachl, T., et al., 2018. Toward global soil moisture monitoring with Sentinel-1: harnessing assets and overcoming obstacles. IEEE Trans. Geosci. Rem. Sens. 57 (1), 520–539. https://doi.org/10.1109/TGRS.2018.2858004.

Bran, D., Ayesa, J., Lopez, C., 2002. Áreas ecológicas de Neuquén. In: Informe Laboratorio De Teledetección-SIG N°4-INTA-EEA Bariloche.

Breiman, L., 2001. Random Forest. Mach. Learn. 45, 5–32. https://doi.org/10.1023/A:1010933404324.

Breiman, L., Cutler, A., Liaw, A., Wiener, M., Liaw, M.A., 2018. Package 'Randomforest', vol. 81. University of California, Berkeley: Berkeley, CA, USA, pp. 1–29.

Brockerhoff, E.G., Jactel, H., Parrotta, J.A., Quine, C.P., Sayer, J., 2008. Plantation forests and biodiversity: oxymoron or opportunity? Biodivers. Conserv. 17 (5), 925–951. https://doi.org/10.1007/s10531-008-9380-x.

Díaz, S., Pascual, U., Stenseke, M., Martín-López, B., Watson, R.T., Molnár, Z., et al., 2018. Assessing nature's contributions to people. Science 359 (6373), 270–272. https://doi.org/10.1126/science.aap8826.

Dong, W., Mitchard, E.T., Chen, Y., Chen, M., Cao, C., Hu, P., et al., 2024. Comparing remote sensing-based forest biomass mapping approaches using new forest inventory plots in contrasting forests in northeastern and southwestern China. https://doi.org/10.48550/arXiv.2405.15438 arXiv preprint arXiv:2405.15438.

Dubayah, R., Blair, J.B., Goetz, S., Fatoyinbo, L., Hansen, M., Healey, S., et al., 2020. The Global Ecosystem Dynamics Investigation: High-resolution laser ranging of the Earth's forests and topography. Science of remote sensing 1, 100002. https://doi.org/10.1016/j.srs.2020.100002.

Dubayah, R.O., Armston, J., Kellner, J.R., Duncanson, L., Healey, S.P., Patterson, P.L., et al., 2022. GEDI L4A Footprint Level Aboveground Biomass Density, Version 2.1. ORNL DAAC, Oak Ridge, Tennessee, USA. https://doi.org/10.3334/ORNLDAAC/2056.

Gasparri, N.I., Baldi, G., 2013. Regional patterns and controls of biomass in semiarid woodlands: lessons from the Northern Argentina Dry Chaco. Reg. Environ. Change 13 (6), 1131–1144. https://doi.org/10.1007/s10113-013-0422-x.

Gregorutti, B., Michel, B., Saint-Pierre, P., 2017. Correlation and variable importance in random forests. Stat. Comput. 27, 659–678. https://doi.org/10.1007/s11222-016-9646-1.

Griscom, B.W., Adams, J., Ellis, P.W., Houghton, R.A., Lomax, G., Miteva, D.A., et al., 2017. Natural climate solutions. Proc. Natl. Acad. Sci. 114 (44), 11645–11650. https://doi.org/10.1073/pnas.1710465114.

Holtgrave, A.K., Röder, N., Ackermann, A., Erasmi, S., Kleinschmit, B., 2020. Comparing Sentinel-1 and-2 data and indices for agricultural land use monitoring. Remote Sens. 12 (18), 2919. https://doi.org/10.3390/rs12182919.

Hua, F., Bruijnzeel, L.A., Meli, P., Martin, P.A., Zhang, J., Nakagawa, S., et al., 2022. The biodiversity and ecosystem service contributions and trade-offs of forest restoration approaches. Science 376 (6595), 839–844. https://doi.org/10.1126/science.abl4649.

Instituto de Botánica Darwinion, IBODA, CONICET. http://www.darwin.edu.ar/ (accessed 14 June, 2025).

IPCC (Intergovernmental Panel on Climate Change), 2014. Climate change, 2014: impacts, adaptation, and vulnerability. Part A: global and sectoral aspects. Contribution of Working Group II to the Fifth Assessment Report of the Intergovernmental Panel on Climate Change. Cambridge University Press, Cambridge, UK.

IPCC (Intergovernmental Panel on Climate Change), 2006. In: Eggleston, H.S., Buendia, L., Miwa, K., Ngara, T., Tanabe, K. (Eds.), 2006 IPCC Guidelines for National Greenhouse Gas Inventories. Elaborado Por El Programa Nacional De Inventarios De Gases De Efecto Invernadero. IGES, Japón.

Körner, C., 1999. Alpine Plant Life: Functional Plant Ecology of High Mountain Ecosystems, vol. 4. Springer, Berlin. https://doi.org/10.1007/978-3-030-59538-8.

Körner, C., 2017. A matter of tree longevity. Science 355 (6321), 130–131. https://doi.org/10.1126/science.aal2449.

Laclau, P., 2003. Biomass and carbon sequestration of ponderosa pine plantations and native cypress forests in northwest Patagonia. For. Ecol. Manag. 180 (1–3), 317–333. https://doi.org/10.1016/S0378-1127(02)00580-7.

Larracy, R., Phinyomark, A., Scheme, E., 2021. Machine learning model validation for early stage studies with small sample sizes. In: 2021 43rd Annual International Conference of the IEEE Engineering in Medicine Biology Society (EMBC). IEEE, pp. 2314–2319. https://doi.org/10.1109/EMBC46164.2021.9629697.

Loguercio, G.A., Simon, A., Winter, A.N., Ivancich, H., Reiter, E.J., Caselli, M., et al., 2024. Carbon density and sequestration in the temperate forests of northern Patagonia, Argentina. Front. For. Glob. Change 7, 1373187. https://doi.org/10.3389/ffgc.2024.1373187.

Luo, H., Ou, G., Yue, C., Zhu, B., Wu, Y., Zhang, X., et al., 2025. A framework for montane forest canopy height estimation via integrating deep learning and multi-source remote sensing data. Int. J. Appl. Earth Obs. Geoinf., 104474 https://doi.org/10.1016/j.jag.2025.104474.

Mendez-Casariego, H., Bran, D.E., Peralta, C.R., Madariaga, M.C., Huerta, G.J., Villarreal, P., et al., 2005. Programa Nacional de Ecorregiones. La región Patagonia: Centros Regionales Patagonia Norte y Patagonia Sur. https://repositorio.inta.gob.ar/handle/20.500.12123/12430.

Moreira, A., Prats-Iraola, P., Younis, M., Krieger, G., Hajnsek, I., Papathanassiou, K.P., 2013. A tutorial on synthetic aperture radar. IEEE Geoscience and remote sensing magazine 1 (1), 6–43. https://doi.org/10.1109/MGRS.2013.2248301.

Movia, C.P., Ower, G.H., Perez, C.E., 1982. Estudio de la vegetación natural de la provincia de Neuquén. Tomo I. Relevamiento (Informe preliminar sujeto a revisión).

Mutanga, O., Masenyama, A., Sibanda, M., 2023. Spectral saturation in the remote sensing of high-density vegetation traits: a systematic review of progress, challenges, and prospects. ISPRS J. Photogrammetry Remote Sens. 198, 297–309. https://doi.org/10.1016/j.isprsjprs.2023.03.010.

Pan, Y., Birdsey, R.A., Phillips, O.L., Houghton, R.A., Fang, J., Kauppi, P.E., et al., 2024. The enduring world forest carbon sink. Nature 631 (8021), 563–569. https://doi.org/10.1038/s41586-024-07602-x.

Paruelo, J.M., Beltran, A., Jobbagy, E., Sala, O.E., Golluscio, R., 1998. The climate of Patagonia: general patterns and controls on biotic processes. Ecol. Aust. 8, 85–101.

Peri, P.L., Gargaglione, V., Pastur, G.M., Lencinas, M.V., 2010. Carbon accumulation along a stand development sequence of *Nothofagus Antarctica* forests across a gradient in site quality in Southern Patagonia. For. Ecol. Manag. 260 (2), 229–237. https://doi.org/10.1016/j.foreco.2010.04.027.

Pötzschner, F., Baumann, M., Gasparri, N.I., Conti, G., Loto, D., Piquer-Rodríguez, M., Kuemmerle, T., 2022. Ecoregion-wide, multi-sensor biomass mapping highlights a major underestimation of dry forests carbon stocks. Remote sensing of environment 269, 112849. https://doi.org/10.1016/j.rse.2021.112849.

R Core Team, 2025. R: a Language and Environment for Statistical Computing. R Foundation for Statistical Computing, Vienna, Austria. https://www.r-project.org/.

Ramírez, C., Correa, M., Figueroa, H., San Martín, J., 1985. Variación del hábito y hábitat de *Nothofagus antarctica* en el centro sur de Chile. Bosque 6 (2), 55–73. https://doi.org/10.4206/bosque.1985.v6n2-01.

Reiter, E.J., Weigel, R., Walentowski, H., Rago, M.M., Simon, A., Pissolito, C., Leuschner, C., 2025. Exotic pine plantations vs. native forests in northern Patagonia: comparing growth patterns and climate change vulnerability. For. Ecol. Manag. 595, 122966. https://doi.org/10.1016/j.foreco.2025.122966.

Richardson, D.M., Rejmánek, M., 2004. Conifers as invasive aliens: a global survey and predictive framework. Divers. Distrib. 10 (5-6), 321–331. https://doi.org/10.1111/j.1366-9516.2004.00096.x.

Silveira, E.M., Radeloff, V.C., Martinuzzi, S., Pastur, G.J.M., Bono, J., Politi, N., et al., 2023. Nationwide native forest structure maps for Argentina based on forest inventory data, SAR Sentinel-1 and vegetation metrics from Sentinel-2 imagery. Rem. Sens. Environ. 285, 113391. https://doi.org/10.1016/j.rse.2022.113391.

Simberloff, D., Nuñez, M.A., Ledgard, N.J., Pauchard, A., Richardson, D.M., Sarasola, M., van Wilgen, B.W., Zalba, S.M., Zenni, R.D., Bustamante, R., Peña, E., Ziller, S.R., 2010. Spread and impact of introduced conifers in South America: lessons from other southern hemisphere regions. Austral Ecol. 35 (5), 489–504. https://doi.org/10.1111/j.1442-9993.2009.02058.x.

Simon, S.M., Glaum, P., Valdovinos, F.S., 2023. Interpreting random forest analysis of ecological models to move from prediction to explanation. Sci. Rep. 13 (1), 3881. https://doi.org/10.1038/s41598-023-30313-8.

Steinke, L.R., Premoli, A.C., Souto, C.P., Hedrén, M., 2008. Adaptive and neutral variation of the resprouter Nothofagus Antarctica growing in distinct habitats in north-western Patagonia. Silva Fenn. 42 (2), 177. https://lup.lub.lu.se/record/1203548.

Tudor, C., Constandache, C., Dinca, L., Murariu, G., Badea, N.O., Tudose, N.C., Marin, M., 2025. Pine afforestation on degraded lands: a global review of carbon sequestration potential. Front. For. Glob. Change 8, 1648094. https://doi.org/10.3389/ffgc.2025.1648094.

Vabalas, A., Gowen, E., Poliakoff, E., Casson, A.J., 2019. Machine learning algorithm validation with a limited sample size. PLoS One 14 (11), e0224365. https://doi.org/10.1371/journal.pone.0224365.

VCS Module VMD 0001, 2013. Redd Methodological Module: Estimation of Carbon Stocks in the above- and Below Ground Biomass in Live Tree and Non-tree Pools (CP-AB). Version 1.1.

Wang, S., Qi, G., Knapp, B.O., 2019. Topography affects tree species distribution and biomass variation in a warm temperate, secondary forest. Forests 10 (10), 895. https://doi.org/10.3390/f10100895.

Xu, L., Lai, H., Yu, J., Luo, S., Guo, C., Gao, Y., et al., 2023. Carbon storage estimation of *Quercus aquifolioides* based on GEDI spaceborne LIDAR data and landsat 9 images in Shangri-La. Sustainability 15 (15), 11525. https://doi.org/10.3390/su151511525.

Zhao, C., Liu, J., Mou, W., Zhao, W., Zhou, Z., Ta, F., et al., 2023. Topography shapes the carbon allocation patterns of alpine forests. Sci. Total Environ. 898, 165542. https://doi.org/10.1016/j.scitotenv.2023.165542.

Zhengchao, R., Huazhong, Z., Hua, S., Xiaoni, L., 2016. Climatic and topographical factors affecting the vegetative carbon stock of rangelands in arid and semiarid regions of China. Journal of Resources and Ecology 7 (6), 418–429. https://doi.org/10.5814/j.issn.1674-764x.2016.06.002.